

## TRACKING THE HIGH-FREQUENCY ENERGY RADIATION SOURCES OF THE 2004 SUMATRA-ANDAMAN $M_W$ 9.0 EARTHQUAKE USING THE SHORT-PERIOD SEISMIC DATA: PRELIMINARY RESULT

HAI-LIN DU\*, LI-SHENG XU<sup>†</sup>, YUN-TAI CHEN<sup>‡</sup>, CHUN-LAI LI  
and KLAUS STAMMLER<sup>§</sup>

*Institute of Geophysics, China Earthquake Administration,  
Beijing 100081, China*

*Seismologisches Zentralobservatorium  
Mozartstr, 57, 91052 Erlangen, Germany*

*\*hailin\_du@hotmail.com*

*†xuls@cea-igp.ac.cn*

*‡chenyt@cea-igp.ac.cn*

*§klaus@szgrf.bgr.de*

Thirty-three stations of short-period seismometers of the Capital Region Digital Seismograph Network, Beijing, China, are organized into an array, and the beam power analysis in time domain is used to track the rupture front of the 2004 Sumatra-Andaman  $M_W$ 9.0 earthquake. The analysis indicates that the earthquake has rupture duration time of 440 s and rupture length of at least 1347 km, and that the rupture started at the initiation point, firstly propagated southward about 160 km with an average rupture velocity of 3.71 km/s, then propagated northward about 1200 km with an average rupture velocity of 2.86 km/s. The success of tracking the rupture front of this earthquake at teleseismic distance further extended the application field of seismic array technique.

### 1. Introduction

A great earthquake occurred off the western coast of northern Sumatra Island at 00:58:53 UTC on December 26, 2004, which generated the most devastating tsunami in recorded history, and eventually resulted in nearly 300,000 fatalities across the Indian Ocean region.<sup>1</sup> The earthquake initiated at 3.3°N, 96.0°E, and at a depth of about 30 km according to the NEIC's determination. The German Regional Seismic Network (GRSN) gave an almost same location for the earthquake, initiating at 3.4°N, 95.8°E.<sup>2</sup>

There have been many studies on this earthquake. The focal mechanism and magnitude were determined.<sup>3-5</sup> The rupture length and width were estimated by various approaches.<sup>1-3,6-8</sup> The duration time was measured by different techniques.<sup>2,4,6,8</sup> The rupture process was imaged by means of various techniques using different types of data.<sup>2,7</sup> The rupture velocities were analyzed and discussed by various methods using different datasets.<sup>8</sup>

Among all the works done so far, as mentioned above, two works are more interesting: one done by Kruger and Ohrnberger<sup>2</sup> and another by Ishii *et al.*<sup>6</sup> Kruger and Ohrnberger<sup>2</sup> modified the standard array-seismological approach and processed the broadband recordings of GRSN for tracking the propagating rupture front. Ishii *et al.*<sup>6</sup> used the Hi-Net seismic array in Japan to map the progression of slip by monitoring the direction of high-frequency radiation. These are for the first time the teleseismic recordings used to track the rupturing trace by means of the array-seismological technique although the similar works had been done in the case of near or local distances.<sup>9-11</sup> In this paper, we apply the moving-window power beam forming technique in time domain to the short-period seismic recordings of the Capital Region Digital Seismograph Network, Beijing, China, and track the propagating rupture front of the 2004 Sumatra-Andaman  $M_W$ 9.0 earthquake. Hopefully, it will be helpful for further understanding the kinematical, even dynamic characteristics of the disastrous earthquakes.

## 2. Data

The Capital Region Digital Seismograph Network (CRDSN) consists of 107 seismic stations, including 59 short-period seismometer stations and 48 broadband seismometer stations. The geometry of the CRDSN is irregular, and the distances between stations vary very much from station to station. To have an array good enough, we choose 33 stations equipped with short-period seismometers and take them as elements of an array as shown in Fig. 1. The station depicted with the bigger triangle was used as the reference station. In this way, the geometry of the array becomes more regular, and the array becomes denser. The aperture of the array is about 200 km. All these instruments have a flat velocity response between 2 Hz and 20 Hz. The distances of the stations from the 2004 Sumatra-Andaman  $M_W$ 9.0 earthquake is about  $40^\circ$ . At these distances the phases PP, PPP, and other secondarily generated phases should be recorded besides P. However, the frequencies of the later phases should be lower than 2 Hz, as pointed by Ni *et al.*<sup>8</sup> We selected the recordings of 600 s from the first arrivals to analyze the propagating rupture front.

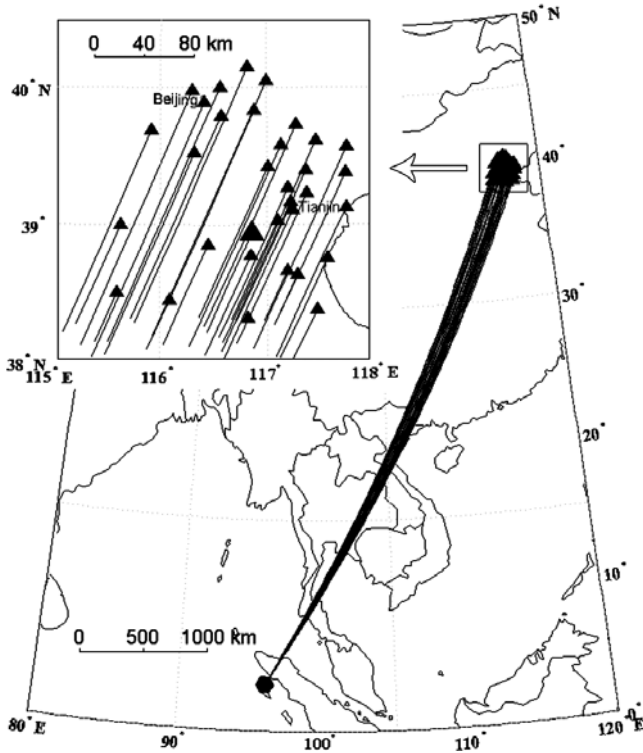


Fig. 1. The epicenter of the 2004 Sumatra-Andaman  $M_W9.0$  earthquake (black hexagon), the locations of the stations of the seismic array (black triangles), and the reference station (the bigger triangle).

### 3. Method

The method of beam power analysis in time domain is used in this study.<sup>12</sup> Here we have a brief description of this method.

A signal arriving at a reference point within the array with horizontal velocity  $v_s$  and a back azimuth  $\theta$  is described as  $s(t)$ . The  $n$ th seismometer with the location vector  $\mathbf{r}_n$ , relative to the array reference point, records the signal  $x_n(t)$ :

$$x_n(t) = s(t - \mathbf{u}_0 \cdot \mathbf{r}_n) \tag{1}$$

where  $\mathbf{u}_0$  is the horizontal slowness vector with:

$$\mathbf{u}_0 = \frac{1}{v_s} (\cos \theta, \sin \theta) \tag{2}$$

The maximum amplitude of the sum of all the recordings of array seismometers is reached as the signals of all stations are in phase, that is, if the time shifts  $\mathbf{u}_0 \cdot \mathbf{r}_n$  disappear. The output of the array can be computed with:

$$y(t) = \frac{1}{N} \sum_{n=1}^N x_n(t + \mathbf{u}_0 \cdot \mathbf{r}_n) \quad (3)$$

for an array of  $N$  elements. For signals with different slowness vector  $\mathbf{u}$  the beam trace is computed as:

$$y(t) = \frac{1}{N} \sum_{n=1}^N s\{t + [(\mathbf{u}_0 - \mathbf{u}) \cdot \mathbf{r}_n]\} \quad (4)$$

The total energy recorded at the array can be calculated by the integration of the squared summed amplitudes over time:

$$E(\mathbf{u} - \mathbf{u}_0) = \int_{-\infty}^{\infty} y^2(t) dt \quad (5)$$

Considering Eqs. (4) and (5), the maximum energy will be reached when  $\mathbf{u} = \mathbf{u}_0$ . In this way, we can have the horizontal slowness of the array reference point.

The relation between slowness and distance is linked with the IASPEI91 earth model.<sup>13</sup> In this way, the locations from where the energy radiates could be determined. For a large earthquake which has a finite fault, seismic recording could be divided into a number of segments by moving time window. The locations determined using the signals within different time windows form the rupture trace of the whole earthquake.

#### 4. Correction for the Slowness Vectors Using Aftershocks

As is known, the slowness vector determined by the array technique is always biased from the truth because of the geometry of the array and/or the heterogeneity of the medium. It is necessary to make correction for the slowness vector directly determined by the data analysis.

The 2004 Sumatra-Andaman  $M_W 9.0$  earthquake was followed by a number of moderate-size aftershocks. Until June 27, 2006, the Capital Region Digital Seismograph Network well recorded 25 aftershocks with magnitudes greater than 5.8. These aftershocks have been well located by

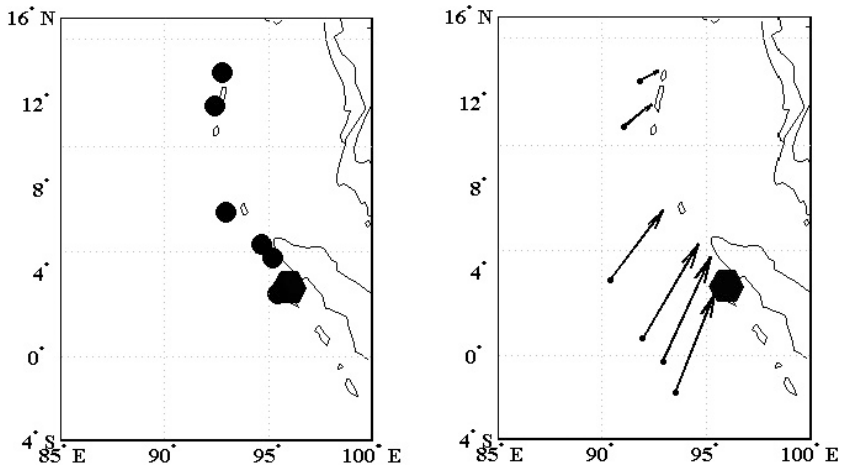


Fig. 2. Locations of the main shock (black hexagon) and the selected aftershocks (black dot) (left). The location correction vectors determined using the seismic recordings of the aftershocks (right).

some institutions such as Harvard University, NEIC, among others, so they could be used to correct the slowness vector in this area. In this study, the locations of the aftershocks published by NEIC were assumed to be correct or true, and compared these with the locations we determine using our approach to have difference vectors for the locations of all the aftershocks. By linear interpolation between any two locations, we could have the difference vectors for all the locations of interests, that is, the locations where the main shock ruptured ran through. Among the 25 aftershocks, we choose six aftershocks which occurred near or on the ruptured region of the main shock as shown on the left panel of Fig. 2, and obtained the corresponding difference vectors as shown on the right panel of Fig. 2. The right panel of Fig. 2 indicates that the different locations (different epicentral distances and/or back azimuth) have different correction vectors (both scales and directions). Using a constant vector to correct all the locations seems to be unreasonable.

## 5. Tracking the Energy Sources

As mentioned above, the first 600s of the initial arrivals were used in this study. The width of the time windows to be shifted is 10s, and the shift step is 4s. Therefore, 150 time windows of the signals are analyzed for

slowness vectors. In finding the solutions, we used the grid-search method. The search step for scalar slowness is  $0.005 \text{ s}/^\circ$ , which yields only distance variations less than 8.6 km at the southern end of the ruptured region and less than 10.4 km at the northern end. The search step for the back azimuth is  $0.07^\circ$ , which yields distance variations less than 5.2 km at the southern end of the ruptured region and less than 4.2 km at the northern end. For each of the time windows, we have one best slowness vector which corresponds to a specific geographic location. In this way, we could have 150 locations for the whole rupture process of the 2004 Sumatra-Andaman  $M_W 9.0$  earthquake, which represent the locations from where high-frequency signals were radiated during the earthquake rupture process. However, the fitness of the beamed signal with the signal recorded at the reference stations became worse when the window was shifted after 440 s. That is the noises were stronger than the source signals after 440 s. Thus to be the duration time of the earthquake is determined to be 440 s. Therefore, the 109 locations determined in the first 440 s are considered to be reliable. The left and right panels of Fig. 3 show the locations before and after being corrected, respectively.

Figure 4 clearly presents the locations where the rupture had gone through, which is from the northwestern shore of the Sumatra Islands to the northeastern shore of the Andaman Islands. The general feature of the rupture geometry fits the trench of islands well. It is very similar to the

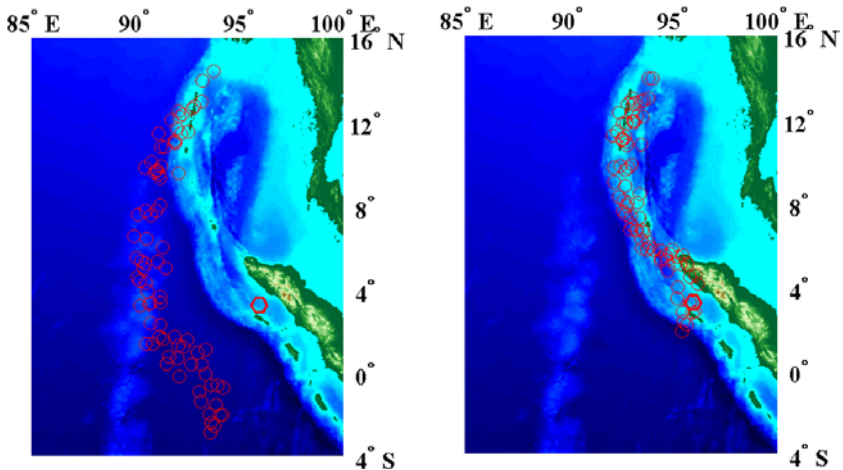


Fig. 3. Locations of high-frequency energy sources before (left) and after (right) being corrected.

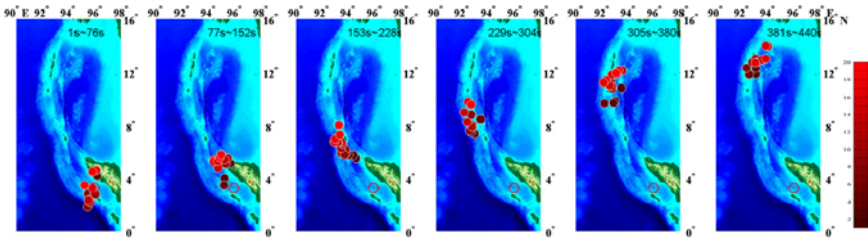


Fig. 4. Snapshots of the progression of rupture front. Each of the snapshots shows the locations of rupture fronts within a time window of 76 s. The solid dots represent the locations of rupture fronts and the open hexagon is the epicenter of the main shock. The color of the dots in the same time window indicates the time progression of rupture fronts.

results obtained by Kruger and Ohrnberger<sup>2</sup> and Ishii *et al.*<sup>6</sup> The rupture length was estimated to be at least 1347 km by calculating the distances between the most northern location and the most southern location. From Fig. 4, we notice that the initial location is not the most southern one indicating that southward rupture occurred. Based on the lengths of rupture toward south and north, respectively, as well as the corresponding times, the average rupture velocities are estimated to be 3.71 and 2.86 km/s.

Figure 4 shows the progression of rupture front. Each of the snapshots shows the rupture spots within a time window of 76 s and in each the color indicates the time order of the ruptured spots. It is clear that overall the rupture initiated at the south, propagated northward, and stopped at the north. More details about the rupture process could be seen in this group of images, but they are preferred to be discussed in the coming paper.

## 6. Discussion and Conclusions

The analysis of the 33 stations recordings indicates that the rupture length of the 2004 Sumatra-Andaman  $M_W 9.0$  earthquake was at least 1347 km. It is much larger than the length suggested by the aftershock distribution<sup>1</sup> and by the analysis of Japanese Hi-Net Array data,<sup>6</sup> also slightly larger than the length of 1200 km suggested by the short-period seismic body waves<sup>8</sup> and the analysis of the Earth's normal modes,<sup>3</sup> and even larger than the length of 1150 km suggested by the analysis of GRSN data.<sup>2</sup>

The analysis suggested that the 2004 Sumatra-Andaman  $M_W 9.0$  earthquake has rupture duration time of 440 s. This is a little shorter than 500 s suggested by the analysis of short-period seismic body waves<sup>8</sup> and

480 s resulted in by the Japanese Hi-Net Array analysis,<sup>6</sup> very close to 430 s suggested by the analysis of GRSN teleseismic data,<sup>2</sup> but much shorter than 600 s yielded by the analysis of Earth's free oscillations.<sup>4</sup>

Our result suggested that the rupture velocities during the earthquake process were variable. Only the average velocity of southward rupture and the average velocity of northward rupture were estimated in this work, which were 3.71 km/s and 2.86 km/s, respectively. These velocities seemed to be larger than those obtained by the analysis of the high-frequency signals<sup>8</sup> and the Japanese Hi-Net Array data.<sup>6</sup>

The array made up of the 33 stations of the Capital Region Digital Seismograph Network, Beijing, China, is good enough for tracking the rupture front of the 2004 Sumatra-Andaman  $M_W$ 9.0 earthquake. The beam power analysis in time domain led to a very similar result to those obtained from the analysis of GRSN broadband recordings<sup>2</sup> and Hi-Net Array short-period recordings<sup>6</sup> clearly and generally describing the progression of rupture front. It is indeed a significant extension of the seismic array technique application besides the application of the local and near-fault recordings.<sup>9–11</sup>

## Acknowledgments

This study is supported by the NSFC (40474018 and 40574025) and the Program of the National Fundamental Research (2004CB418404-4 and 2001CB711005), and the Joint Foundation of Earthquake Science (A07047). Contribution No. of IGCEA: 07FE3004.

## References

1. T. Lay, H. Kanamori, C. J. Ammon, M. Nettles, S. N. Ward, R. C. Aster, S. L. Beck, S. L. Bilek, M. R. Brudzinski, R. Butler, H. R. DeShon, G. Ekstrom, K. Satake and S. Sipkin, *Science* **308** (2005) 1127.
2. F. Krüger and M. Ohrnberger, *Nature* **435** (2005) 937.
3. S. Stein and E. A. Okal, *Nature* **434** (2005) 581.
4. J. Park, T. A. Song, J. Tromp, E. Okal, S. Stein, G. Roullet, E. Clevede, G. Laske, H. Kanamori, P. Davis, J. Berger, C. Breitenberg, M. V. Camp, X. Lei, H. P. Sun, H. Z. Xu and S. Rosat, *Science* **308** (2005) 1139.
5. M. K. Giovanni, S. L. Beck and L. Wagner, *Geophys. Res. Lett.* **29** (2002) 2018, doi: 10.1029/2002GL015774.
6. M. Ishii, P. Shearer, H. Houston and J. Vidale, *Nature* **435** (2005) 933.

7. C. J. Ammon, C. Ji, H. Thio, D. Robinson, S. D. Ni, V. Hjorleifsdottir, H. Kanamori, T. Lay, S. Das, D. Helmberger, G. Ichinose, J. Polet and D. Wald, *Science* **308** (2005) 1133.
8. S. Ni, H. Kanamori and D. Helmberger, *Nature* **434** (2005) 582.
9. P. Spudich and E. Cranswick, *Bull. Seismol. Soc. Am.* **74** (1984) 2083.
10. P. Goldstain and R. J. Archuleta, *J. Geophys. Res.* **96** (1991) 6187.
11. B. S. Huang, *Geophys. Res. Lett.* **28** (2001) 3377.
12. S. Rost and C. Thomas, *Rev. Geophys.* **40**(3) (2002) 1.
13. B. L. N. Kennett and E. R. Engdahl, *Geophys. J. Int.* **105** (1991) 429.